# A Method of Validating and Verifying the Digital Model of the Vibratory Bowl Feeder

Van-Mui Nguyen, Anh-Tuan Hoang, Ha-Manh Nguyen, Dung-Tien Nguyen

Department of Mechatronics, Faculty of Mechanical Engineering, University of Economic and Technical Industries

*Corresponding author email: nvmui @ uneti.edu.vn

*Abstract*— *In modern day production, vibratory bowl feeders have become a popular option for the provision of discrete parts with light weight and small size. The numerical model for determining the movement of workpieces on the bowl has been applied to give the corresponding designs of vibratory bowl structure and workpieces needed. However, there is still a big difference between theory and practice, which results in a lot of post-fabrication time for commissioning and calibration of control parameters, and manufacture may not be possible due to errors, or the design method cannot maximize device performance. This paper presents a numerical model based on MSC ADAMS that demonstrates the workpieces delivery process by vibration. In other words, the test can be performed in a digital environment but still reflects the real conditions of the experiment process. The numerical model has been tested and verified to be similar to the actual device of the vibratory bowl feeder. This simulation model can be used to find the optimal parameter of the vibratory bowl feeder before manufacturing equipment*

*Keywords*— *Numerical model, vibratory bowl feeders, MSC ADAMS, validation, verification.*

## I. INTRODUCTION

Bowl feeder vibrating and feeding systems are often used for workpieces with small weight and size. This device is commonly used in automatic assembly lines [1–4]. The general structure and principle of the device is shown in Figure 1. It consists of a bowl (1) mounted on the upper vibrator (2). The upper vibrator (2) is placed on top of the three leaf springs (3), which perform revolving movements back and forth around the vertical axis, whereby the workpiece moves along the trough on the bowl. The electromagnets (4) and leaf springs (3) create movements for the sorting bowl to vibrate. Normally the electromagnet consists of two parts, one is fixed with the lower vibrator (5) and the other is coiled, the rest fixed to the upper vibrator (2) and moved with the upper vibrator (2) and the bowl. The current in the coil creates a magnetic force between the two parts of the electromagnet by the act of attracting and discharging between the two parts of the magnet. This force creates the movement of the workpiece on the bowl. The force between the two parts of the magnet is controlled by varying the voltage from the control box (7). Cushion rubber (6) works to suppress system vibrations affecting other devices. The velocity of the workpiece moving on the bowl depends on the bowl's amplitude.



| | |
|---|---|
| 1. | Bowl |
| 2. | Upper bowl |
| 3. | Leaf spring |
| 4. | Electromagnet |
| 5. | Lower vibrator |
| 6. | Cushion rubber |
| 7. | Control box |

Fig. 1. Automatic vibratory bowl feeder

Typically, vibrating workpiece feeders are designed according to modular design. Structural elements such as cushion rubber, upper vibrator, electromagnets, vibration sources, etc. are available. Particularly, the vibration bowl is designed and manufactured for each different type of workpiece, then fabricated, installed and calibrated to find the optimal parameters. Some previous studies were based on theoretical and pragmatic studies by analyzing workpieces kinetic factors [4], [5]. Or use the dynamics model of a degree of freedom [6] to calculate the bowl's specific vibration frequency. Or use a three-step order model to accurately determine the vibration frequency and the influence of cushion rubber [4], [7]. Some authors have studied the deformation of the spring, the effect of leaf springs on the workpieces movement [1], [5], [8], [9] The deformation of the spring is studied as: deformation in transverse direction and axial direction with no torsional strain included [6]. Other studies [2], [10–12] also analyze workpieces movement analysis through numerical and experimental models. The states of the workpieces are also confirmed between the element model and the experimental model. Generally, the vibrating bowl is driven by the sinusoidal oscillating electromagnetic forces. When changing the voltage, the amplitude of oscillation also changes.

In this study, finite element method is used to show the theoretical functions used to show that the oscillations that make the motion for the bowl are sinusoidal. Through experiments to determine vibration amplitude and angular amplitude. From the established function put into numerical simulation environment. The results of numerical simulations are verified through real models.

## II. NUMBERICAL MODEL

When the workpiece moves on the trough, it has a state of sliding and jumping [2], [10], [13] meaning that the workpiece moves in contact with the trough and its relative motion and is under the influence of kinetic friction. In this process, the gutter can move downward, so the workpiece will fall freely in

18

![IJSES logo]

*International Journal of Scientific Engineering and Science*
*Volume 4, Issue 4, pp. 18-23, 2020.*                        *ISSN (Online): 2456-7361*

the moving cycle. There is an elastic collision that will occur when the workpiece falls into the trough.

By examining the movement of the workpiece along the circumference of the bowl, a comparison between the friction of the bowl wall and the workpiece and the friction between the guide path and the workpiece can be made. Assuming that, during the movement of the workpiece on the guide track, the friction between the bowl wall and the workpiece is negligible and can be ignored. Schematic analysis of workpiece force is as follows:
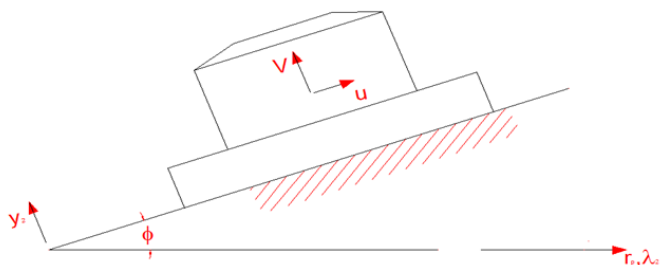


Fig. 2. Coordinates of workpiece on the guide trough

To analyze the movement of the workpiece, establish a coordinate system with the parallel parallel to the surface of the guide chute as u, the right angle as v. For a bowl with radius $r_p$. The original position of the bowl is Y (u, v) and it moves to the position Y1 (u1, v1) of the motion equation:

$$u_1 = \lambda_1 r_p cos\phi + y_1 \sin\phi$$

$$v_1 = -\lambda_1 r_p \sin\phi + y_1 cos\phi \quad (1)$$

The coordinates of bowls $y_1$ and $\lambda_1$ are functions of vector Y (vertical displacement and rotation of the bowl).

We have the coordinates of the bowl determined based on the coordinates of the base $(y_2, \lambda_2)$ and the displacement of leaf spring d, $r_1$ as the radius of the base:

$$y_1 = y_2 + d cos\theta \quad (2)$$

$$\lambda_1 = \lambda_2 + \frac{d}{r_1}\sin\theta \quad (3)$$

Replace (2) and (3) in (1) we have:

$$\begin{bmatrix} u_1 \\ v_1 \end{bmatrix} = \begin{bmatrix} \sin\phi & r_p cos\phi\left(\dfrac{r_p}{r_1}\sin\theta cos\phi + cos\theta \sin\phi\right) \\ cos\phi & r_p \sin\phi\left(\dfrac{r_p}{r_1}\sin\theta \sin\phi + cos\theta cos\phi\right) \end{bmatrix} Y \quad (4)$$

When moving on the trough it is in relatively contact and slippery state so we have:

$$\ddot{u}_p = \mu_k(\ddot{v}_1 + g cos\phi) - g\sin\phi$$

$$\ddot{v}_p = \ddot{v}_1 \quad (5)$$

Where $\mu_k$ is the friction coefficient between workpiece and trough.

We see that the workpiece movement is influenced by a harmonic force.

## III. ESABLISING AN EXPERIMENTAL MODEL FOR DETERMINING THE VIBRATION AMPLITUDE

### 3.1. Experimental model and the process of getting results

The experimental model (Figure 3) uses two IN-085 proximity sensors of Bruel & Kjaer Vibro. The first sensor is mounted vertically to measure the displacement of the bowl vertically. The second sensor is mounted tangentially to the bowl to measure the tangential displacement.
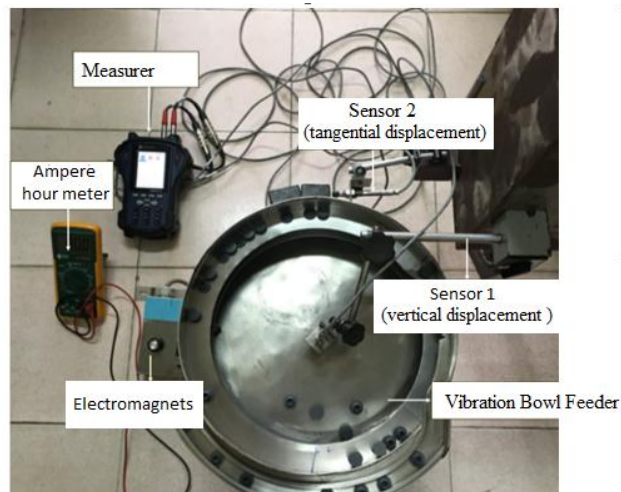


Fig. 3. Experimental model for determining the vibration amplitude

Experiments were conducted at different voltage levels. From the experimental results through ReX software to determine the amplitude of oscillation. Figure 4, shows that at a voltage of 170V, the vertical displacement reaches a value of 396x2 = 792µm, the tangential displacement is 102x2 = 204µm.
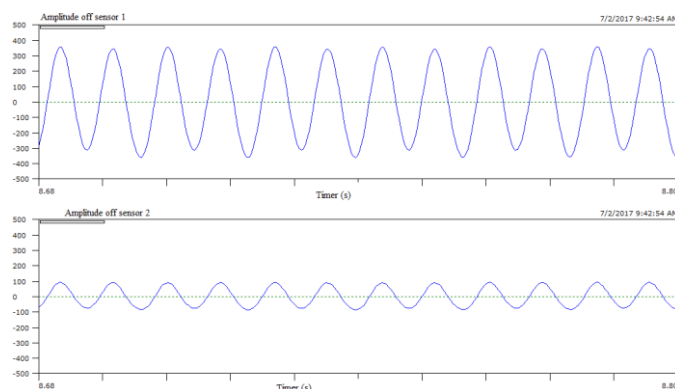


Fig. 4. Data processing at 170V

### 3.2. Constructing voltage-dependent kinematic functions

We see that the first sensor mounted vertically measures and results in the displacement of the bowl vertically or in other words it is the amplitude of the oscillation of the bowl.

This is the amplitude of the kinetic function oscillating in a straight line. The result of processing data of the second sensor is that the amplitude fluctuates in a tangential way, we have to determine the rotation angle of the bowl or the angular amplitude of the dynamic function. Diagram and definition as follows:
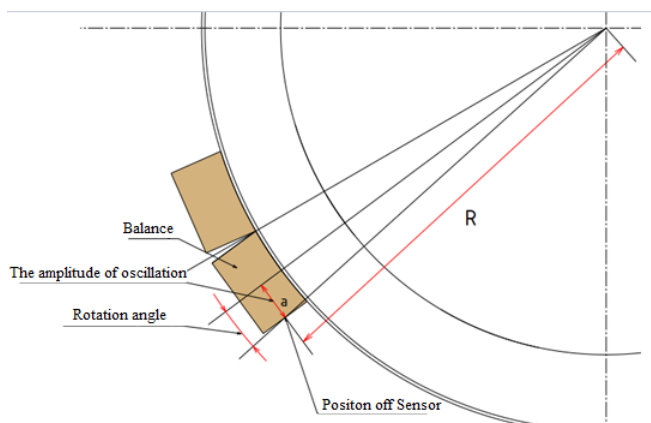
19

Fig. 5. Diagram for calculating the rotation angle (angular amplitude)

$$Rotation\ angle \approx \tan\frac{a}{R} \quad (6)$$

Where

a: The amplitude of oscillation is determined by sensors measuring horizontally

R: Distance from sensor to the center of the bowl

Experiments are conducted at different voltage levels. From the experimental data, combined with the calculation, the author gets the following results:

Table 1. The translational amplitude value and rotation angle are determined experimentally

| No | Voltage (V) | Amplitude of rotation angle | Translational amplitude | Kinematic functions |
|----|-------------|-----------------------------|-------------------------|---------------------|
| 1 | 90 | 0.012 | 0.0115 | $\alpha = 0,012\sin(2\pi.100.t)$ |
| | | | | $x = -0,0115\sin(2\pi.100.t)$ |
| 2 | 100 | 0.017 | 0.015 | $\alpha = 0,017\sin(2\pi.100.t)$ |
| | | | | $x = -0,015\sin(2\pi.100.t)$ |
| 3 | 110 | 0.022 | 0.0191 | $\alpha = 0,022\sin(2\pi.100.t)$ |
| | | | | $x = -0,0191\sin(2\pi.100.t)$ |
| 4 | 120 | 0.0285 | 0.0246 | $\alpha = 0,0285\sin(2\pi.100.t)$ |
| | | | | $x = -0,0246\sin(2\pi.100.t)$ |
| 5 | 130 | 0.037 | 0.032 | $\alpha = 0,037\sin(2\pi.100.t)$ |
| | | | | $x = -0,032\sin(2\pi.100.t)$ |
| 6 | 140 | 0.048 | 0.0413 | $\alpha = 0,048\sin(2\pi.100.t)$ |
| | | | | $x = -0,0413\sin(2\pi.100.t)$ |
| 7 | 150 | 0.0645 | 0.0553 | $\alpha = 0,0645\sin(2\pi.100.t)$ |
| | | | | $x = -0,0553\sin(2\pi.100.t)$ |
| 8 | 160 | 0.0845 | 0.0698 | $\alpha = 0,0845\sin(2\pi.100.t)$ |
| | | | | $x = -0,0698\sin(2\pi.100.t)$ |
| 9 | 170 | 0.0985 | 0.0855 | $\alpha = 0,0985\sin(2\pi.100.t)$ |

## IV. VERIFICATION AND CONFIRMATION OF NUMERICAL MODELS

To simulate the system in a digital environment, the author built an automatic workpiece delivery system based on MSC ADAMS. This software allows engineers to study the dynamics of moving mechanisms, how load and forces are distributed across the mechanical system and optimizing mechanical product performance.

ADAMS makes it easy to create and test virtual prototypes of mechanical systems in a short time at a much lower cost than physical construction and testing. Unlike most CAD tools, ADAMS incorporates physical elements of the parts. At the same time, it is possible to solve dynamic, static, semi-static and dynamic equations quickly and accurately.

We see that the movement of the vibratory bowl under the influence of the electromagnetism of the magnet consists of two movements that are fluctuating up and down and rotating around the axis of the spring system as well as the bowl [1], [8], [14] Therefore, in ADAMS simulation environment we also have to attach kinematic functions to the bowl's oscillation. The kinematic functions here are sinusoidal oscillating functions, so the vertical oscillation and swing oscillation must be determined. Experimental model is made according to Figure 3.

### 4.1. Equations of motion

Consider a vacant bottle-shaped workpiece moving on the trough (Figure 2). We have the kinetic energy when moving on the trough is:

$$T = \frac{1}{2}(m\dot{u}^2 + m\dot{v}^2 + I\dot{\phi}^2) \quad (7)$$

Where m and I are the mass and rotational inertia of the workpiece, respectively.

20

Considering on the vertical axis Y, we have the potential of the workpiece determined:

$$V = mgv \tag{8}$$

Where g is the gravitational acceleration.
Subtract (7) minus (8) we have

$$L = T - V \tag{9}$$

It is called the Lagrangian function of the dynamical system. With a multi-object dynamics system, the Lagrangian function is written as follows:

$$L = \sum_{j=1}^{N} T_j - V_j \tag{10}$$

In which Tj and Vj are kinetic and potential energy respectively of a system consisting of N objects. In this paper, research is shown only in the case of an workpiece, ie N = 1.

According to Lagrangian's law, the motion function of a multi-object kinetic system is determined by the function:

$$\frac{d}{dt}\left(\frac{\partial L}{\partial \dot q}\right) - \frac{\partial L}{\partial q} + \Phi_q^T \lambda = Q \tag{11}$$

$$q = \begin{Bmatrix} u \\ v \\ \phi \end{Bmatrix} \tag{12}$$

Where $(12)$ is the coordinate matrix. The matrix q contains all the coordinates of the mechanisms that make up the system. Then we have a matrix of n rows.

$$\frac{\partial L}{\partial q} = \begin{pmatrix} \frac{\partial L}{\partial q_1} \\ \frac{\partial L}{\partial q_2} \\ \vdots \\ \frac{\partial L}{\partial q_n} \end{pmatrix} \tag{12}$$

Similarly, we have $\frac{\partial L}{\partial \dot q}$ is a matrix of n rows and 1 column.

Each element $\frac{\partial L}{\partial q}$ demonstrates the sensitivity of the Lagrangian function for the machine system to the one that creates its motion. The components of $\frac{\partial L}{\partial \dot q}$ is the derivative over time of workpiecegenesis

$$\Phi_q = \frac{\partial \Phi}{\partial q} \tag{13}$$

Jacobian matrix

The second derivative of the kinetic components of the workpiece in the two directions u and u have.

$$p_u = \frac{\partial L}{\partial \dot u} = m\dot u \ \text{và} \ p_v = \frac{\partial L}{\partial \dot v} = m\dot v \tag{14}$$

Similar to rotation we have: $p_\theta = \frac{\partial L}{\partial \dot\theta} = I\dot\theta \tag{15}$

With momentum for any coordinates q we have:

$$p_q = \frac{\partial L}{\partial \dot q} \tag{16}$$

If q is any displacement coordinates with coordinates u or v then the time derivative equation (16) is obtained as below :

$$\frac{d}{dt}\left(\frac{\partial L}{\partial \dot q}\right) = \dot p_q = m\ddot q \tag{17}$$

If q is the coordinate of rotation angle, we have:

$$\frac{d}{dt}\left(\frac{\partial L}{\partial \dot q}\right) = \dot p_q = I\ddot q \tag{18}$$

From (9) we combine with (17) and (18) :

$$\frac{d}{dt}\left(\frac{\partial L}{\partial \dot q}\right) - \frac{\partial L}{\partial q} = \begin{pmatrix} m\ddot u \\ m\ddot v \\ I\ddot\theta \end{pmatrix} + \begin{pmatrix} 0 \\ mg \\ 0 \end{pmatrix} \tag{19}$$

Substituting (19) and Lagrange (7) we have.

$$\begin{pmatrix} m & 0 & 0 \\ 0 & m & 0 \\ 0 & 0 & I \end{pmatrix} \begin{pmatrix} \ddot u \\ \ddot v \\ \ddot\theta \end{pmatrix} + \begin{pmatrix} 0 \\ mg \\ 0 \end{pmatrix} + \Phi_q^T = Q \tag{20}$$

For any coordinate, in a two- or three-dimensional coordinate system, equation $\frac{d}{dt}\left(\frac{\partial L}{\partial \dot q}\right) - \frac{\partial L}{\partial q}$ solved in ADAMS is like being solved in three dimensional coordinate system. In the general case equation (20) becomes:

$$M\ddot q + \dot M\dot q - \frac{1}{2}\dot q^T \frac{\partial M}{\partial q}\dot q + \frac{\partial V}{\partial q} + \Phi_q^T \lambda = Q \tag{21}$$

M: is the mass matrix

$\frac{1}{2}\dot q^T \frac{\partial M}{\partial q}\dot q$: total kinetic energy of the system

V: potential energy

$\Phi_q^T$: Jacobian matrix mxn refers to the links between elements

Q: the matrix that shows the force exerted in a one-column and n-row matrix.

*4.2. Experiment, validation and verification digital models*

According to equation (21), we find that there are many factors affecting the movement of the workpiece in the bowl such as friction coefficient, vibration amplitude, input voltage, torsional groove angle ... [1][2]. From there, building a simulation model with functions of voltage as inputs (vibration amplitude along vertical and torsion axis). Compare results between experiment and simulation to confirm the numerical model.

For a function table based on empirical amplitude and rotation values (Table 1). We proceed to enter the function value into the simulation according to the translation and rotation functions. Checking the amplitude value on the numerical model, we have the following table of comparison of values:

Table 2. Compare the value of translational amplitude and rotation angle between experiment and numerical simulation

| No | Voltage (V) | Rotational angle (degree) | | | Translational amplitude (mm) | | |
|---|---|---|---|---|---|---|---|
| | | Calculation | Simulation | Amount of deflection | Calculation | Simulation | Amount of deflection |
| 1 | 90 | 0.012 | 0.0108 | 0.0012 | 0.0115 | 0.010 | 0.0015 |
| 2 | 100 | 0.017 | 0.0152 | 0.0018 | 0.015 | 0.0135 | 0.0015 |
| 3 | 110 | 0.022 | 0.0192 | 0.0028 | 0.0191 | 0.0179 | 0.0012 |
| 4 | 120 | 0.0285 | 0.0252 | 0.0033 | 0.0246 | 0.0235 | 0.0011 |
| 5 | 130 | 0.037 | 0.0345 | 0.0025 | 0.032 | 0.0305 | 0.0015 |
| 6 | 140 | 0.048 | 0.0440 | 0.0040 | 0.0413 | 0.0393 | 0.002 |
| 7 | 150 | 0.0645 | 0.0614 | 0.0031 | 0.0553 | 0.0527 | 0.0026 |
| 8 | 160 | 0.0845 | 0.0822 | 0.0023 | 0.0698 | 0.0654 | 0.0044 |
| 9 | 170 | 0.0985 | 0.0925 | 0.0060 | 0.0855 | 0.0803 | 0.0052 |

The experiment was conducted at different voltage levels and taking the average value over the five measurements, we obtained the average velocity of the experiment.

Table 3. Velocity values determined experimentally

| No | Voltage (V) | Velocity (mm/s) | | | | | Average velocity (mm/s) |
|---|---|---|---|---|---|---|---|
| | | 1st | 2nd | 3rd | 4th | 5th | |
| 1 | 90 | 3.55 | 3.58 | 3.56 | 3.60 | 3.56 | 3.57 |
| 2 | 100 | 5.62 | 5.66 | 5.65 | 5.65 | 5.64 | 5.65 |
| 3 | 110 | 8.49 | 8.53 | 8.52 | 8.50 | 8.49 | 8.51 |
| 4 | 120 | 17.31 | 17.23 | 17.24 | 17.29 | 17.28 | 17.27 |
| 5 | 130 | 30.09 | 30.15 | 30.12 | 30.08 | 30.21 | 30.13 |
| 6 | 140 | 45.70 | 45.77 | 45.75 | 45.76 | 45.72 | 45.74 |
| 7 | 150 | 71.48 | 71.50 | 71.40 | 71.43 | 71.39 | 71.44 |
| 8 | 160 | 106.84 | 106.77 | 106.90 | 106.87 | 106.82 | 106.84 |
| 9 | 170 | 133.13 | 133.40 | 133.32 | 133.12 | 133.88 | 133.37 |

With the experimental model using measuring instrument and calculation, we get a table of measurement results and calculation of the kinematic function parameters (Table 1). From numerical simulation we can determine the velocity of the workpieces with different voltage levels.

Table 4. Table of comparing velocity by experiment and by numerical simulation

| No | Voltage (V) | Velocity (mm/s) | | Amount of deflection | |
|---|---|---|---|---|---|
| | | Experimental model | Numerical model | (mm/s) | % |
| 1 | 90 | 3.57 | 3.86 | 0.29 | 8.12 |
| 2 | 100 | 5.65 | 5.10 | 0.55 | 9.73 |
| 3 | 110 | 8.51 | 8.64 | 0.13 | 1.53 |
| 4 | 120 | 17.27 | 16.17 | 1.10 | 6.37 |
| 5 | 130 | 30.13 | 28.01 | 2.12 | 7.04 |
| 6 | 140 | 45.74 | 44.37 | 1.37 | 2.99 |
| 7 | 150 | 71.44 | 72.94 | 1.50 | 2.10 |
| 8 | 160 | 106.84 | 108.94 | 2.10 | 1.97 |
| 9 | 170 | 133.37 | 134.86 | 1.49 | 1.12 |

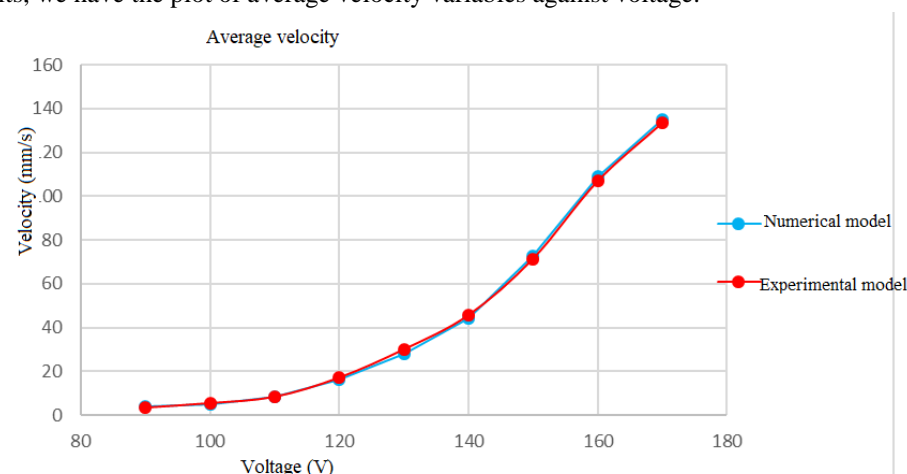With the above results, we have the plot of average velocity variables against voltage.



Fig.6. Plot of average velocity variables against voltage.

From the graph in Figure 6 we see that there is a similarity between the numerical model and the experimental model.

The deviation in velocity value ranges from 0.13 to 2.12 (mm / s), which is equivalent to 1.12 to 9.3%. So the numerical model reflects correctly and is similar to the real model.

## V.    CONCLUSION

Numerical simulation of kinetic processes of workpieces in the bowl was presented and confirmed by experimental data. The results show that the movement velocity of the workpiece (workpiece production capacity) between numerical and experimental environment is similar.

Experimentally validating the numerical model has achieved the required results (deviation <10%) when assessing the influence of voltage (vibration and rotation amplitude) on the velocity of the workpiece.

With the above results, it is possible to apply the multi-object dynamic simulation environment (numerical simulation environment) in optimizing the dynamic parameters as well as calculating, designing, manufacturing, testing or manufacturing devices.

## REFERENCES

[1]  E. Mucchi, R. Di Gregorio, and G. Dalpiaz, "Elastodynamic analysis of vibratory bowl feeders: Modeling and experimental validation," Mech. Mach. Theory, (2011).

[2]  I. HAN and Y. LEE, "Chaotic Dynamics of Repeated Impacts in Vibratory Bowl Feeders," J. Sound Vib, 249 (3) (2002) 529–541.

[3]  S. B. Choi and D. H. Lee, "Modal analysis and control of a bowl parts feeder activated by piezoceramic actuators," J. Sound Vib.275 (1–2) (2004) 452–458.

[4]  R. Silversides, J. S. Dai, and L. Seneviratne, "Force analysis of a vibratory bowl feeder for automatic assembly," J. Mech. Des. Trans. ASME, 127 (4) (2005) 637–645

[5]  X. Ding and J. S. Dai, "Characteristic equation-based dynamics analysis of vibratory bowl feeders with three spatial compliant legs," IEEE Trans. Autom. Sci. Eng, 5 (1) (2008) 164–175.

[6]  S. Okabe and A. Y. Yokoyama, "Study on Vibratory Feeders: Calculation of Natural Freq uency of Bowl-Type Vibratory Feeders," J. Manuf. Syst,103, (January 1981) (1981) 249–256.

[7]  G. P. Maul and M. Brian Thomas, "A systems model and simulation of the vibratory bowl feeder," J. Manuf. Syst, 16 (5) (1997) 309–314.

[8]  T. V. Địch, "Tự động hóa quá trình sản xuất," Nhà xuất bản Khoa học và Kỹ thuật, (2006)

[9]  P.C.P. Chao and C.Y. Shen, "Dynamic modeling and experimental verification of a piezoelectric part feeder in a structure with parallel bimorph beams," Ultrasonics, (2007)

[10]  E. M. Sloot and N. P. Kruyt, "Theoretical and experimental study of the transport of granular materials by inclined vibratory conveyors," Powder Technol, 87 (3) (1996) 203–210.

[11]  N. V. Mui and L. G. Nam, "Ứng dụng mô phỏng số trong đánh giá sự ảnh hưởng của tần số rung đến các thông số động học của phôi trong hệ thống cấp phôi tự động theo nguyên lý kích rung," Hội nghị Cơ học kỹ thuật toàn quốc, 1 (2014) 149–154.

[12]  N. V. Mui and L. G. Nam, "Đánh giá sự ảnh hưởng của góc nghiêng đường dẫn hướng đến các thông số động lực học của phôi trong hệ thống cấp phôi tự động theo nguyên lý rung động bằng mô phỏng số," Hội nghị cơ khí toàn quốc, (2015).

[13]  L. Han and J. X. Gao, "A Study on the Modelling and Simulation of Part Motion in Vibratory Feeding," Appl. Mech. Mater, 34–35, (2010) 2006–2010.

[14]  G. N. T. H. Nguyễn Phương, "Cơ sở tự động hóa trong ngành Cơ khí," Nhà xuất bản Khoa học và Kỹ thuật, (2005).

[15]  "Intro Adams Theory," (1997).